Electromagnetic response and approximate SO(5) symmetry in high-T_c superconductors

C. P. Burgess and J. M. Cline
Physics Department, McGill University, 3600 University Street, Montréal, Québec, Canada H3A 2T8

C. A. Lütken
Physics Department, University of Oslo, P.O. Box 1048, Blindern, N-0316 Norway

(Received 20 August 1998)

It has been proposed that the effective Hamiltonian describing high T_c superconductivity in cuprate materials has an approximate SO(5) symmetry relating the superconducting (SC) and antiferromagnetic (AF) phases of these systems. We show that robust consequences of this proposal are potentially large optical conductivities and Raman scattering rates in the AF phase, due to the electromagnetic response of the doubly charged pseudo Goldstone bosons which must exist there. This provides potentially strong constraints on the properties of the bosons, such as their mass gap and velocity, at any given value of the doping. [S0163-1829(98)52046-2]

It has recently been proposed[1] that the antiferromagnetic (AF) and superconducting (SC) phases of the high-T_c cuprates are related by an SO(5) symmetry, a suggestion which has both stimulated considerable interest[2–5] and drawn sharp criticism.[6,7] Both the interest and the criticism are inspired by the central role played by the symmetry relating the two phases.

The SO(5) picture has much to recommend it. It gives a simple and concrete qualitative understanding of many features of the cuprates, as well as predicting brand new phenomena, such as superconducting vortices having antiferromagnetic cores[3] and persistent superconducting phase correlations within the AF phase.[4] On the negative side, Anderson and Baskaran have argued that such a finite-dimensional symmetry description of the cuprates is inconsistent with the electron localization properties of the two phases.[7]

In this work we exploit another strength of the SO(5) theory—namely, its predictive power—to bring further evidence to the discussion. A model-independent consequence of the SO(5) picture is the existence in the AF phase of an electrically charged pseudo-Goldstone boson (pGB) quasiparticle, whose dispersion relation and low-energy couplings are tightly constrained by the SO(5) symmetry.[1,5] We use these to compute the contribution of these quasiparticles to the electromagnetic response of the cuprate materials in the AF phase. In particular we find the Raman scattering rate and the real part of the far-infrared conductivity, which turn out to be potentially comparable to or larger than what is experimentally observed, depending on how badly SO(5) becomes broken as one moves away from optimal doping into the underdoped region. We emphasize that our calculation relies almost exclusively on the assumed SO(5) symmetry, and depends only minimally on the microscopic details of these systems.

The key tool in the analysis is the effective Lagrangian density which describes the electromagnetic couplings of the SO(5) pGB's. This can be written as

$$\mathcal{L}=|[\partial_t-2ie(\mu+A_0)]\phi|^2-\sum_i\left|v_i^{\phi}\left(\nabla_i-\frac{2ie}{c}A_i\right)\phi\right|^2$$
$$+(\partial_t\vec{n})^2-\sum_i\,(v_i^n\nabla_i\vec{n})^2-V(\phi,\vec{n}). \qquad (1)$$

Here μ is the chemical potential which describes the system's doping, A_i is the electromagnetic gauge potential, and v_i^{ϕ} and v_i^n are the pGB velocities, which can differ along the three principal directions of the medium. In the limit of exact SO(5) symmetry, we would have $v_i^n=v_i^{\phi}\equiv v_i$, and the scalar potential $V(\phi,\vec{n})$ satisfying $V=V(|\phi|^2+\vec{n}^2)$.

There are two important, but conceptually very different, regimes to which this Lagrangian may apply.

(1) Deep within the AF or SC phases, where fluctuations in the modulus $|\phi|^2+\vec{n}^2$ are negligible, V becomes a constant in the SO(5) symmetry limit, and ϕ and $\vec{n}$ describe the dynamics of the Goldstone and pseudo-Goldstone quasiparticles. For instance, for the AF phase there are four such modes: two gapless magnons with dispersion relation $E_n^2(p)=\Sigma_i(v_i^n p_i)^2$, and two pGB's with charge $\pm 2e$ and dispersion $[E_{\phi}(p)\mp 2e\mu]^2=\varepsilon_g^2+\Sigma_i(v_i^{\phi}p_i)^2$. Approximate SO(5) invariance amounts to the statement that $|v_i^{\phi}-v_i^n|$ is small compared to v_i, and the gap, ε_g, is much smaller than the typical microscopic scale of the system, $J\sim 0.1$ eV. ''Much smaller'' here means of comparable size to the experimentally measured 41 meV gap,[8] which is interpreted within the SO(5) context as a pGB of the SC phase.[9] Here the two-dimensional nature of the cuprates dictates the sum on i runs only over the two spatial derivatives (x and y) which label the copper-oxygen planes.

(2) Near the critical boundaries between the various phases, $\mathcal{L}$ plays the role of a Ginzburg-Landau (GL) free energy, and (in mean field theory) V may be expanded to quartic order: $V=-m_{\phi}^2|\phi|^2-\frac{1}{2}m_n^2|\vec{n}|^2+\lambda_{\phi}|\phi|^4+2\lambda_{\phi n}|\phi|^2|\vec{n}|^2+\lambda_n|\vec{n}|^2$. In this case the model can be two or three dimensional (but anisotropic, $v_z\neq v_x=v_y$) depending on how close one is to the critical limit. SO(5) invariance

implies in this case $m_\phi^2 = m_n^2$ and $\lambda_\phi = \lambda_n = \lambda_{n\phi}$, and so approximate SO(5) invariance is the statement that the deviations from these relations are systematically small. Phenomenology requires $m_n^2 > m_\phi^2$ when the doping is sufficiently small, in order that the ground state of the system be AF, with $\phi = 0$ and $\vec{n} \neq 0$. In this regime the pseudo-Goldstone gap in the AF phase may be computed, giving $\varepsilon_g^2 = -m_\phi^2 + (\lambda_{\phi n}/\lambda_n) m_n^2$, which clearly vanishes in the SO(5) limit, as required.

Numerical studies of t-J and Hubbard models which support the SO(5) picture indicate that SO(5) is only expected to be a good symmetry in the vicinity of the critical doping, between the AF and SC phases.[10] The key question, which we would like to subject to experimental scrutiny, is *how far* away from the phase boundary does the approximate symmetry hold? In what follows we will show that the chemical potential must be large near this boundary, in order to suppress the electromagnetic signatures of charged pseudo-Goldstone bosonic excitations on the AF side. It then becomes difficult to understand why approximate SO(5) should persist rather far into the SC phase, for larger dopings, as proponents of the SO(5) picture envision.

The existence of charged bosons with a small gap has strong observable consequences for the optical conductivity and Raman scattering properties in the AF phase. These predictions are quite robust. The interaction of the photons with the bosons, the first two terms of Eq. (1), is completely fixed by electromagnetic gauge invariance. The self-interactions described by the other terms, including possible higher powers of $|\phi|$ not shown, must vanish for Goldstone bosons in the limit of zero energy and exact SO(5) symmetry, and so may be treated perturbatively for low energies and approximate symmetry. These also ensure the small size of the gap, ε_g.

Conductivity. We start with the contribution of the charged pseudo-Goldstone quasiparticle to the real part of the conductivity, σ_1, within the AF phase. This is proportional to the imaginary part of the photon self-energy due to a virtual pseudo-Goldstone boson loop, and related to the rate at which the pGB's are pair produced by incident photons. Our result agrees in the appropriate limits with closely analogous formulas for the electromagnetic response of a hot pion gas.[11] For pGB's which can move in three dimensions, and whose velocity is much less than that of light, we obtain

$$\sigma_{1,\mathrm{i}} = \frac{e^2}{24\pi\hbar\lambda}\left(\frac{v_i^2 c}{v_x v_y v_z}\right)\left(1 - \frac{4\varepsilon_g^2}{\hbar^2\omega^2}\right)^{3/2}\left[1 + N_B\left(\frac{\omega}{2}\right)\right], \tag{2}$$

where the absorbed light of wavelength λ is polarized in the ''i'' direction, taken to be one of the crystal axes. (See Fig. 1.) (Henceforth we drop the superscript ϕ from the pGB velocities v_i.) $N_B(\omega) = n_+(\omega) + n_-(\omega)$, where $n_\pm(\omega) = 1/\{\exp[(\hbar\omega \pm \mu)/kT] - 1\}$ is the usual Bose-Einstein statistics factor, and $e^2/\hbar = 2.4341 \times 10^{-4}\ \Omega^{-1}$. This contribution to the conductivity vanishes for photons whose energy $\hbar\omega$ is below the threshold $2\varepsilon_g$ for producing two pGB's. The corresponding absorption coefficient is given by $\sigma_{1,\mathrm{i}}/(\epsilon_0 c)$, where $\epsilon_0 c = 2.654 \times 10^{-3}\ \Omega^{-1}$.

To take into account that the pGB's may be confined to move in the superconducting planes, we have also computed

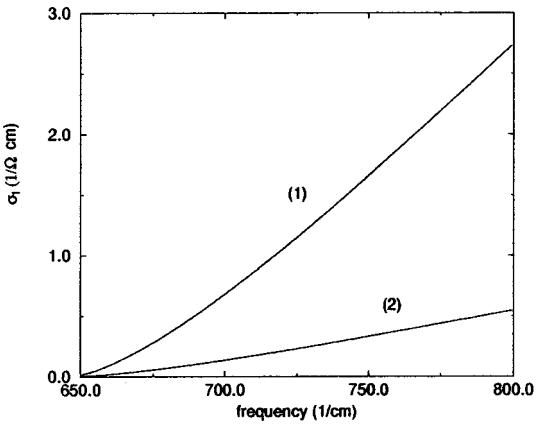

FIG. 1. The optical conductivity σ_1 as a function of the photon energy ω, in units of $\Omega^{-1}\ \mathrm{cm}^{-1}$, for two different pGB velocities, (1) $v/c = 2 \times 10^{-4}$, and (2) $v/c = 10^{-3}$. The other relevant parameters are $\varepsilon_g = 0.04$ eV, $T = 300$ K, and $\mu = 0$.

σ_1 using the lattice dispersion relation $E = \{v_\perp^2 p_\perp^2 + [2v_z \sin(ap_z/2)/a]^2 + \varepsilon_g^2\}^{1/2}$, integrating p_z between $\pm\pi/a$, where a is the spacing between the planes. Defining $\eta = 1 - \frac{1}{2}(a/v)^2(\omega^2 - \varepsilon_g^2/\hbar^2)$, the phase space integral can be done exactly, giving

$$\sigma_{1,i} = \frac{e^2}{16\pi^2\hbar a}\left(\frac{v_i v_z}{v_\perp a\,\omega}\right)^2\left[1 + N_B\left(\frac{\omega}{2}\right)\right] G_i(\eta), \tag{3}$$

where $G_\perp(\eta) = \sqrt{1-\eta^2} - \eta\cos^{-1}\eta$ and $G_z(\eta) = \frac{1}{2}(\cos^{-1}\eta - \eta\sqrt{1-\eta^2})$ (these become, respectively, $-\pi\eta$ and $\pi/2$ for $\eta < -1$). The continuum approximation on which the 3D equation (2) is based is valid when $a \to 0$ (so $\eta \to 1$). For the parameters of interest, we find that the 3D formula is practically indistinguishable from Eq. (3), although the difference starts to become apparent for frequencies greater than $800\ \mathrm{cm}^{-1}$.

How large are these results? If the gap is approximately $\varepsilon_g = 0.04$ eV as suggested by the neutron scattering data, the interplane spacing is $a = 0.5$ nm, and using the magnon speed $v_i = 2 \times 10^{-4} c$,[12] then for $\omega = 0.1$ eV (frequency $= 800\ \mathrm{cm}^{-1}$) and $T = 0.025$ eV (300 K), $\sigma_1 = 2.75\ \Omega^{-1}\ \mathrm{cm}^{-1}$. This is more than three times larger than the measured values of $\sigma_1 < 1\,\Omega^{-1}\ \mathrm{cm}^{-1}$ for the undoped cuprate $Sr_2CuO_2Cl_2$, as reported in Ref. 13; moreover, the frequency dependence disagrees with the data, which has σ_1 decreasing in this frequency range. Although the perturbative treatment of the pGB's begins to break down at higher energies, if we can trust our results at somewhat higher energies of $\omega = 0.5$ eV ($= 4000\ \mathrm{cm}^{-1}$), then σ_1 grows to $100\ \Omega^{-1}\ \mathrm{cm}^{-1}$, in even greater conflict with measured values near $1\ \Omega^{-1}\ \mathrm{cm}^{-1}$ in the materials Gd_2CuO_4 and $YBa_2Cu_3O_6$.[13] (Reference 14 has also measured conductivities, but their maximum frequency of $700\ \mathrm{cm}^{-1}$ may be below the threshold $2\varepsilon_g$ needed for production of pGB pairs.)

Although the magnitude and the shape of σ_1 suggest a conflict between SO(5) and experiments, there are several caveats. One is that σ_1 is inversely proportional to the pGB velocity, v_i, which is not precisely known. The other is that our computation is only valid for energies within the domain of approximation of the low-energy pGB Lagrangian used

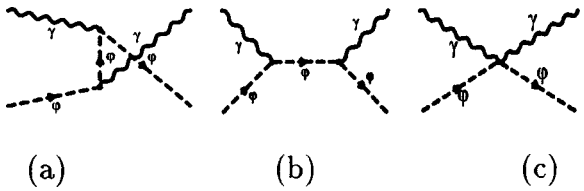

FIG. 2. The Feynman graphs which describe photon-pGB scattering.

here, i.e., for $\omega \ll J \sim 0.1$ eV. Above these energies the pGB's need not contribute as a weakly coupled and comparatively narrow state. The experimental constraints happen to be strongest just in the region where our long-wavelength approximation starts to break down. Thus we turn to another possible signal of the pGB electric response.

Raman Scattering. We now consider the contribution to the Raman scattering rate, coming from Compton-like photon scattering from the pseudo-Goldstone quasiparticles in the sample. The Feynman graphs for this process are those of Fig. 2.

We work in a gauge for which the expression for the scattering amplitude, $\mathcal{M}$, is particularly simple. That is, if $p^{\mu}_{i,f}$ and $k^{\mu}_{i,f}$ denote the initial and final pGB and photon four-momenta, respectively, and we choose the photon polarizations, $\tilde{\epsilon}^{\mu}_{i,f}$, to satisfy $\tilde{\epsilon}_i \cdot (2\tilde{p}_i + \tilde{k}_i) = \tilde{\epsilon}_f \cdot (2\tilde{p}_i - \tilde{k}_f) = 0$, then diagrams (a) and (b) of the Fig. 2 vanish, leaving an amplitude of the form $\mathcal{M}_{ab} = 4e^2 \tilde{\epsilon}^{(a)}_i \cdot \tilde{\epsilon}^{(b)}_f$. We use here the convenient notation for any four-vector, in which a tilde indicates the multiplication of the spatial components by the corresponding velocity, v_i. That is, $\tilde{p}_0 = p_0$, and $\tilde{p}_i = v_i p_i$.

Let us assume that the initial photon is moving in the z direction, perpendicular to the superconducting planes, and the final one is scattered by 180°, as is the case in the experiments to which we compare. Assuming the x-y plane to be isotropic, $v_x = v_y = v_\perp$, and averaging over initial and summing over final polarizations leads to the following expression (temporarily setting $\hbar = c = 1$):

$$\mathcal{S} \equiv \frac{1}{2} \sum_{a,b} |\mathcal{M}_{ab}|^2 = 8e^4 v_\perp^4 [1 + (1-A)^2], \tag{4}$$

where $A = (1+v_z^2) v_\perp^2 p_\perp^2 / (D_i D_f)$, with

$$D_i = E_i - v_z^2 p_{i,z} + \frac{1}{2} \omega_i (1 - v_z^2), \tag{5}$$

$$D_f = E_i + v_z^2 p_{i,z} - \frac{1}{2} \omega_f (1 - v_z^2). \tag{6}$$

Conservation of four-momentum constrains the initial and final boson energies and momenta according to

$$E_i = \frac{\Delta\omega}{2} + \omega_0 v_z f(p_\perp); \quad p_{i,z} = -\omega_0 - \frac{\Delta\omega}{2 v_z} f(p_\perp)$$

$$E_f = -\frac{\Delta\omega}{2} + \omega_0 v_z f(p_\perp); \quad p_{f,z} = \omega_0 - \frac{\Delta\omega}{2 v_z} f(p_\perp), \tag{7}$$

where $\Delta\omega = \omega_f - \omega_i$, $\omega_0 = (\omega_i + \omega_f)/2$, and

$$f(p_\perp) = \left(1 + \frac{\epsilon_g^2 + v_\perp^2 p_\perp^2}{|v_z^2 \omega_0^2 - \Delta\omega^2/4|} \right)^{1/2}. \tag{8}$$

Care must be taken with these expressions, however, because the quantity A can diverge for some value of $p_\perp$. In a general gauge this comes about when the virtual boson in Fig. 2(b) goes on its mass shell. [Equivalently, the gauge transformation which we used to remove Fig. 2(b) becomes singular for these momenta.] We handle this situation, when it arises, by including the width of the pGB itself. This may be done by adding a small imaginary part, $i\Gamma/2$, to the boson energies in the definition of A, giving a finite scattering rate. We find our results to be insensitive to reasonable values such that $\Gamma \leqslant \epsilon_g$, for relevant temperatures and energies.

The observable of interest is the differential scattering rate per unit sample thickness, l, per unit incident laser power, I: $R = (1/I)(d\Gamma/dl)$. This is the quantity which does not depend on the details of the target or of the incident photon flux. We compute the differential rate of such scattering into a solid angle $d\Omega$ (centered about 180°), and into a final energy interval $d\omega_f$, $\mathcal{R} = dR/d\omega_f d\Omega$. We then do the thermal average over the initial and final pGB's, sum over the final photon polarizations, and average over the initial ones. This assumption that the incident photons are unpolarized, and scattered-photon polarizations are not detected, simplifies our expressions, but is not crucial for the result. We find

$$\mathcal{R} \equiv \frac{\omega_f}{(4\pi)^4 v_\perp^2 \omega_i^2 |\Delta\omega|} \sum_{\pm} \int dp_z n_\pm(E_i)[1 + n_\pm(E_f)] \mathcal{S},$$

where $n_\pm$ is the Bose-Einstein distribution function with chemical potential $\pm\mu$. The limits of integration are found by varying $p_\perp^2$ between 0 and ∞ in Eq. (7) for $p_{i,z}$, and $p_\perp^2$ in the integrand is determined in term of $p_{i,z}$ by inverting the same equation. As a function of the final photon energy, the rate is peaked near $\omega_f = \omega_i$, with an approximate maximum value of

$$\mathcal{R}_{\max} \cong \left(\frac{\alpha v_\perp}{\pi v_z \omega} \right)^2 T e^{-\beta(\epsilon_g - |\mu|)}, \tag{9}$$

using the Boltzmann approximation for the distribution functions. Kinematics constrains the scattered photon energy to lie in the narrow range $(1-v_z)/(1+v_z) < \omega_f/\omega_i < (1+v_z)/(1-v_z)$. For visible light (500 nm) and $v = 10^{-3} c$, this gives a half-width of 40 cm^{-1} in the frequency ν. In Fig. 3 we show $\mathcal{R}$ for representative input values $\omega_i = 2$ eV, $T = 93$ K, $\epsilon_g = 0.04$ eV, $\mu = 0$, and 0.01 eV, $\Gamma = 0.1\epsilon_g$, and optimistically large velocities $v_z = v_\perp = 10^{-3} c$. For these numbers we find rates of order $\mathcal{R} \sim (150 - 300)$ cps/mW/Å/steradian/eV, with a smooth, featureless line shape. For optical photons the penetration depth of typical samples is of order 100 Å,[15] leading to a prediction of 10^4 events/mW/Å/sr/eV in the backward direction. Experimentally, the observed rate for the compound Bi2212 is only 15 cps/mW/Å/sr/eV. However this must be corrected[16] for detector efficiency (0.1) and surface losses (0.1−0.01), which in the worst case would bring the predicted value into agreement with the experiments.

We point out that the predicted rate is exponentially dependent on the ratio of the pGB gap or chemical potential to the temperature because of the Boltzmann factor in Eq. (9).

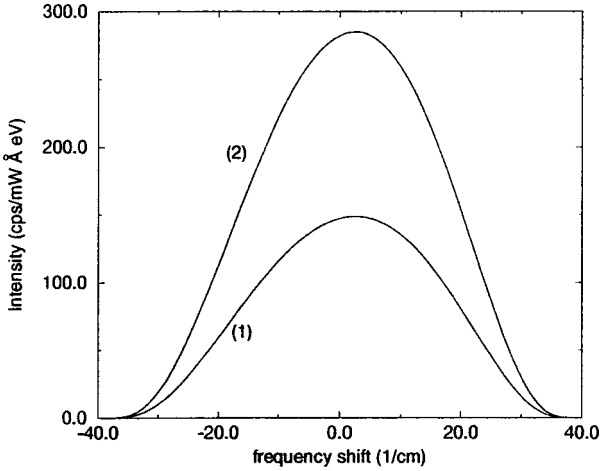

FIG. 3. The differential Raman scattering rate $\mathcal{R}$ as a function of the photon frequency shift $\nu_i - \nu_f$, in units of cm^{-1}. The curves correspond to (1) the parameters given in the text, and (2) same as (1) except with nonzero chemical potential, $\mu = 0.01$ eV.

If $(\varepsilon_g - |\mu|) \lesssim kT$, there is a further gain by a factor of 150 in the rate, which would cause a serious discrepancy between the predicted and observed values. On the other hand, the width depends linearly on the pGB velocity. If $v < 2 \times 10^{-4} c$, this width becomes less than the experimental resolution of Ref. 15, which only measures Raman shifts greater than $\sim 10/\mathrm{cm}$.

Similarly to the conductivity, the Raman scattering rate near zero shift depends only weakly on whether the pGB's are allowed to move in three dimensions or confined to the 2D planes, for the parameters of interest. By repeating the above calculation using the lattice dispersion relation for the pGB's, one finds that the continuum version is a good approximation when $\omega a \ll c$, rather than the condition $\omega a \ll v$ which applied for the conductivity. Although we are interested in larger frequencies in Raman scattering than for the conductivity, the latter condition is still satisfied, and the differences between the 2D and 3D Raman intensities are small.

In conclusion, we have used SO(5) symmetry to compute the low-energy contribution of the electrically charged pseudo-Goldstone bosons to the electromagnetic response of cuprates doped to be antiferromagnets. We find measurably large conductivities and Raman scattering rates, due to the presence of electrically charged states with a comparatively small gap. At present the dispersion relation of the putative bosons is not sufficiently well known to rule out SO(5) for the cuprates based on the data. It is encouraging, however, that the conductivity and Raman intensities have a complementary dependence on the pGB velocity, so that one or the other should show evidence for the pGB's, especially if the experiments are improved, e.g., Raman scattering at frequency shifts less than 10/cm.

We thank R. Hackl and T. Timusk for information about the experiments, and C. Gale and A. Berlinksy for useful discussions.

[1] S.-C. Zhang, Science **275**, 1089 (1997).

[2] S. Rabello, H. Kohno, E. Demler, and S. C. Zhang, Phys. Rev. Lett. **80**, 3586 (1998); C. L. Henley, *ibid.* **80**, 3590 (1998); C. P. Burgess, J. Cline, R. B. MacKenzie, and R. Ray, Phys. Rev. B **57**, 8549 (1998); E. Demler, H. Kohno, and S.-C. Zhang, *ibid.* **58** 5719 (1998); D. Scalapino, S.-C. Zhang, and W. Hanke, *ibid.* **58**, 443 (1998).

[3] D. P. Arovas, A. J. Berlinsky, C. Kallin and S.-C. Zhang, Phys. Rev. Lett. **79**, 2871 (1997).

[4] E. Demler, A. J. Berlinsky, C. Kallin, G. B. Arnold, and M. R. Beasley, Phys. Rev. Lett. **80**, 2917 (1998).

[5] C. P. Burgess and C. A. Lütken, cond-mat/9611070 (unpublished); Phys. Rev. B **57**, 8642 (1998).

[6] M. Greiter, Phys. Rev. Lett. **79**, 4898 (1997); cond-mat/9705282 (unpublished); E. Demler, S. C. Zhang, S. Mexiner, and W. Hanke, Phys. Rev. Lett. **79**, 4937 (1997).

[7] G. Baskaran and P. W. Anderson, cond-mat/9706076 (unpublished); R. Laughlin, cond-mat/9709195 (unpublished); P. W. Anderson and G. Baskaran, cond-mat/9711197 (unpublished).

[8] H. A. Mook *et al.*, Phys. Rev. Lett. **70**, 3490 (1993).

[9] E. Demler and S.-C. Zhang, Phys. Rev. Lett. **75**, 4126 (1995); cond-mat/9705191 (unpublished).

[10] R. Eder, W. Hanke, and S.-C. Zhang, Phys. Rev. B **57**, 13 781 (1998); W. Hanke *et al.*, cond-mat/9807015 (unpublished).

[11] C. Gale and J. I. Kapusta, Nucl. Phys. B **357**, 65 (1991); A. I. Titov, T. I. Gulamov, and B. Kämpfer, Phys. Rev. D **53**, 3770 (1996).

[12] J. M. Tranquada and G. Shirane, Phys. Rev. B **40**, 4503 (1989); S. M. Hayden *et al.*, *ibid.* **54**, R6905 (1996).

[13] D. B. Tanner *et al.*, Proc. SPIE **2696**, 13 (1996).

[14] C. C. Homes and T. Timusk, cond-mat/9509128 (unpublished).

[15] R. Hackl, G. Krug, R. Nemetschek, M. Opel, and B. Stadlober, Proc. SPIE **2696**, 194 (1996).

[16] R. Hackl (private communication).